

Charging and infrared spectroscopy of self-assembled quantum dots in a magnetic field

Arkadiusz Wojs

*Institute for Microstructural Sciences, National Research Council of Canada, Ottawa, Canada K1A 0R6
and Institute of Physics, Technical University of Wrocław, Wybrzeże Wyspiańskiego 27, 50-370 Wrocław, Poland*

Paweł Hawrylak

Institute for Microstructural Sciences, National Research Council of Canada, Ottawa, Canada K1A 0R6

(Received 1 December 1995)

The few-electron states of the lens-shaped self-assembled quantum dots in the magnetic field are studied. The calculated charging and infrared absorption spectra reflect the magnetic-field-induced transitions between different states of interacting electrons. The theoretical results compare well with recent experiments by Drexler *et al.* [Phys. Rev. Lett. **73**, 2252 (1994)]. New features are predicted to occur at higher magnetic fields.

I. INTRODUCTION

Drexler *et al.*¹ have recently reported capacitance and infrared absorption measurements of charged self-assembled $\text{In}_x\text{Ga}_{1-x}\text{As}/\text{GaAs}$ quantum dots in a magnetic field. The dots containing as few as ~ 6 confined states were charged with electrons filling the s -like and the p -like electronic shells. The infrared spectroscopy was used to study the electronic excitations of the dots as a function of the number of electrons and magnetic field.

The form and shape of self-assembled dots (SAD's) depend on growth conditions.² Dots in the shape of pyramids,^{3,4} disks,⁵ and lenses² were reported, although the actual determination of the shape is not definite. The SAD's described here are the lens-shaped hills spontaneously formed on a narrow $\text{In}_x\text{Ga}_{1-x}\text{As}$ wetting layer (WL) and surrounded by the GaAs barriers.^{1,2,6} The actual shape of the dot is modeled as a part of a sphere with a fixed diameter at the base and the height-to-diameter ratio reported to be ≈ 0.12 .⁶⁻⁸ Electrons confined to the WL quantum well are localized in the area of the dot where their energy is lowered due to increased thickness of the $\text{In}_x\text{Ga}_{1-x}\text{As}$ layer.

II. SINGLE-ELECTRON STATES

The electronic states of small SAD's in a magnetic field are very accurately approximated by the Fock-Darwin (FD) states of an infinite parabolic potential.⁹ The dependence of the electronic energy spectrum on the size of the dot and on the height of the confining potential has been reported elsewhere.⁹ The results presented here correspond to the parameters given by Drexler *et al.*,¹ i.e., dot diameter 200 Å and indium fraction 0.5, yielding the 350-meV discontinuity in the conduction band at the $\text{In}_{0.5}\text{Ga}_{0.5}\text{As}/\text{GaAs}$ interface. The parameters of the materials forming the SAD enter through the effective electron mass m_e and dielectric constant ϵ , which include all effects of strain, discontinuities in the effective mass, and dielectric constant, etc.

The comparison of the magnetic-field evolution of exact eigenenergies (dots) and the FD energy levels (lines) corresponding to the confining energy $\omega_0=50$ meV has been shown in Fig. 1. The exact eigenenergies for a given angular

momentum R have been calculated numerically for the confining potential reflecting the actual shape of the SAD.⁹ The number of confined states in the zero field is 3 ($R=0, \pm 1$) and there is also a strong resonance above the bottom of the WL continuum (not marked in the figure). With increasing magnetic field one can observe that the state with $R=2$ (initially the resonance) lowers its energy and becomes bound around 5 T. Since the confining energy is very high, appropriately strong fields are necessary to bring this ($R=2$) state below the one with $R=-1$ (crossing at 20.5 T) and eventually reach the magnetic quantization limit with a clearly developed structure of distinct Landau levels. The spin splitting is negligible even for high magnetic fields (~ 0.03 meV/T) and has not been indicated in the figure.

III. FEW-ELECTRON STATES

In order to calculate the few-electron states we shall approximate the actual single-electron spectrum with the FD

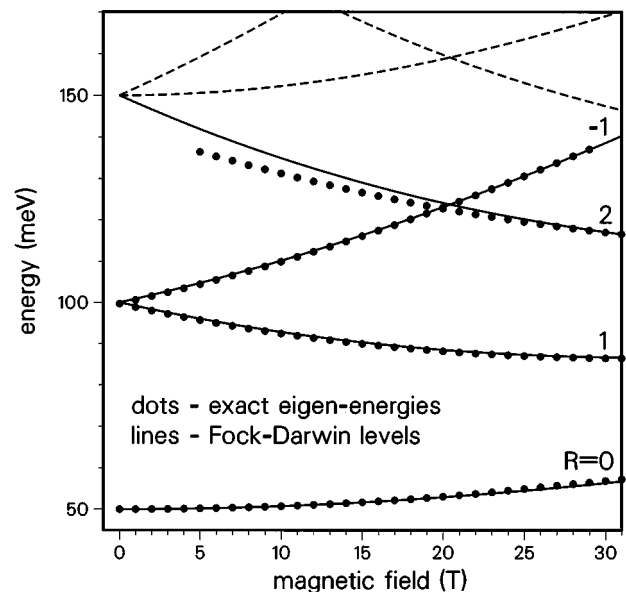


FIG. 1. Exact energy levels of SAD's (dots) and Fock-Darwin levels (lines) as a function magnetic field. Solid lines correspond to the states included in the basis for diagonalization of the many-electron Hamiltonian.

states. The FD states $|nm\rangle = (a^\dagger)^n (b^\dagger)^m |00\rangle / \sqrt{n!m!}$ are those of a pair of harmonic oscillators with the eigenfrequencies $\Omega_\pm = 1/2(\Omega \pm \omega_c)$, where $\Omega^2 = \omega_0^2 + 4\omega_c^2$ and $\omega_c = eB/cm_e$ is the cyclotron frequency. Associating the index n with the frequency Ω_+ and the index m with the frequency Ω_- , the energy E_{nm} and orbital angular momentum R_{nm} of the state $|nm\rangle$ are $R_{nm} = m - n$ and $E_{nm} = \Omega_+(n + 1/2) + \Omega_-(m + 1/2)$.

The many-body Hamiltonian given in the second quantization reads

$$\begin{aligned}
 H = & \sum_{n,m,\sigma} (E_{nm} + g\mu_B B\sigma) c_{nm\sigma}^\dagger c_{nm\sigma} \\
 & + \frac{1}{2} \sum_{n_1,m_1,\sigma_1} \sum_{n_2,m_2,\sigma_2} \langle n'_1 m'_1; n'_2 m'_2 | V_{ee} | n_2 m_2; n_1 m_1 \rangle \\
 & \quad \times c_{m'_1 n'_1 \sigma_1}^\dagger c_{m'_2 n'_2 \sigma_2}^\dagger c_{m_2 n_2 \sigma_2} c_{m_1 n_1 \sigma_1}, \quad (1)
 \end{aligned}$$

where $c_{nm\sigma}^\dagger$ ($c_{nm\sigma}$) are the operators creating (annihilating) an electron with the spin σ in the FD state $|nm\rangle$, V_{ee} is the electron-electron Coulomb repulsion, and $g\mu_B B\sigma$ is the Zeeman energy. The two-body Coulomb matrix elements $\langle n'_1 m'_1; n'_2 m'_2 | V_{ee} | n_2 m_2; n_1 m_1 \rangle$ in the FD basis are given elsewhere.¹⁰ The Coulomb interaction conserves the total angular momentum R and the z th component of the total spin S hence the diagonalization of the Hamiltonian (1) is performed separately for each (R, S_z) subspace.

The basis of the few-electron Hilbert space is constructed from the properly antisymmetrized products of single-electron FD states (including spin σ) $|n_1 m_1 \sigma_1; n_2 m_2 \sigma_2; \dots; n_N m_N \sigma_N\rangle \equiv \hat{A} \prod_{i=1}^N |n_i m_i\rangle |\sigma_i\rangle$. For each value of magnetic field the lowest four FD states are kept (these are the levels plotted with the solid line in Fig. 1, corresponding to actually confined states and the $R=2$ resonance at low fields) and all higher ones are disregarded. The mixing between confined FD states and the WL continuum is neglected. However, the presence of the continuum is automatically included through the fitting of the effective confining energy ω_0 to the exact single-electron energies.

In Fig. 2 we have plotted the ground-state (GS) energies of the interacting N -electron systems. The curves corresponding to different N have been vertically shifted so that all of them can be shown in a single frame. The zero-field GS energies have been marked on the vertical axis and the arrow in the top-left corner gives the vertical scale common to all curves. The pairs of numbers in parentheses (total angular momentum, total spin) $= (R, S)$ indicate the GS configurations. Since the characteristic interaction energy $\langle 00; 00 | V_{ee} | 00; 00 \rangle \approx 30$ meV is lower than the characteristic confining energy $\omega_0 = 50$ meV, the many-body GS's are dominated by the lowest-kinetic-energy configurations. A mixing of different electronic shells is weak. The major effect of the interaction is therefore the blueshift of the noninteracting energy levels by the interaction (weakly depending on the field). This is no longer true for partially filled shells where Coulomb interactions and spin play a major role.

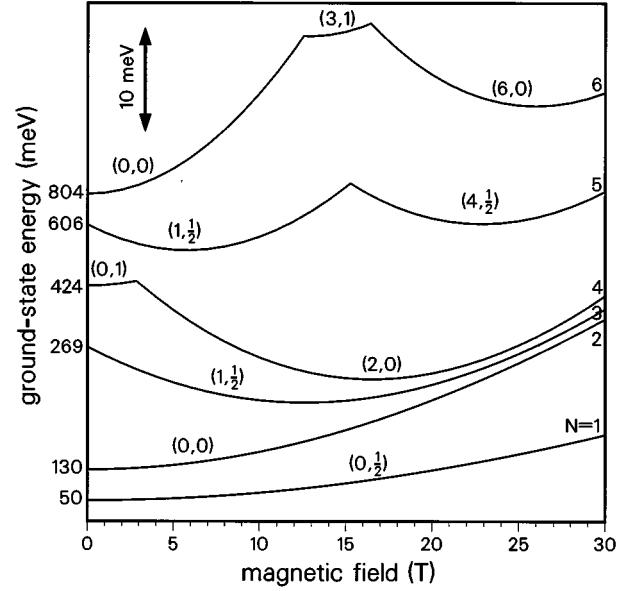


FIG. 2. Ground-state energies of the many-electron systems as a function of the magnetic field. The curves have been vertically shifted to fit in the frame: the energies in the zero field are indicated on the vertical axis and the scale common for all curves is given in the top-left corner. Configurations of the states (R, S) have also been shown.

The GS's of $N=1, 2$, and 3 electrons are almost purely the lowest-kinetic-energy noninteracting states: $|00\downarrow\rangle$, $|00\downarrow; 00\uparrow\rangle$ and $|00\downarrow; 00\uparrow; 01\downarrow\rangle$, respectively. The spin polarization and further transitions between the “magic” angular-momenta states^{11,12} for two- and three-electron states take place well above 30 T.

The first magnetic-field-induced transition in the GS takes place for $N=4$ electrons, i.e., two electrons in a partially filled p shell. For low magnetic fields the two electrons on the half-filled second shell take advantage of the degeneracy of the two FD orbitals ($|01\rangle$ and $|10\rangle$) and maximize their total spin $S=1$ (satisfying Hund's rule) to lower their energy by an exchange-interaction term $\langle 01; 10 | V_{ee} | 01; 10 \rangle$. In non-zero fields the degeneracy of the second shell is removed and the kinetic energy of the maximum spin configuration increases. At $B \approx 2.8$ T the gain in exchange energy is overtaken by an increase of kinetic energy and the system reverts to a spin singlet $S=0$ lower-kinetic-energy configuration.

The transition in the $N=5$ electron system at 15 T corresponds to changing of the FD orbital by the outer electron (from $|10\rangle$ into $|02\rangle$) in the presence of the rigid four-electron core. It occurs earlier than the FD levels actually cross since the new many-body state has lower interaction energy. In case of six electrons there are two GS transitions as the two electrons successively change the FD orbital $|10\rangle$ into $|02\rangle$.

IV. CHARGING OF THE DOT

The GS energy of the interacting electrons in the quantum dot can be probed by means of the single-electron capacitance spectroscopy (SECS).^{11,12} SECS measures the increased capacitance of an $(N-1)$ -electron dot due to the

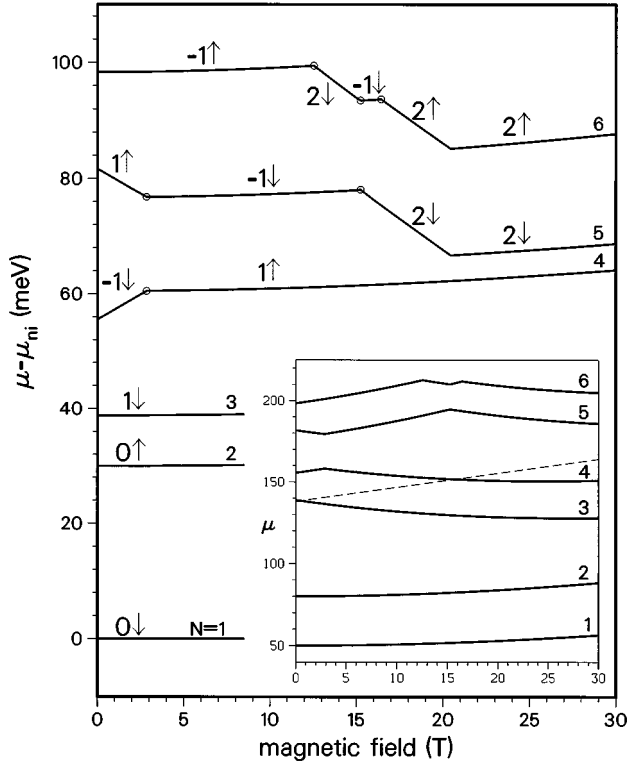


FIG. 3. Charging energies (difference in the chemical potential due to interaction) of the SAD's as a function of the magnetic field. The angular momenta and spins of orbitals into which the electron is added are indicated. The inset shows the chemical potential.

addition of a single electron from a distant metallic electrode. The charging takes place when the chemical potential of the reservoir (electrode), controlled by the applied gate voltage, equals the chemical potential of the dot $\mu(N)$. The chemical potential $\mu(N) = E_{GS}(N) - E_{GS}(N-1)$ is the difference in the ground-state energy of the dot due to addition of a single electron. Recently, Drexler *et al.*¹ reported SECS experiments for the SAD, where charging of the dot with at least four electrons has been demonstrated.

In Fig. 3 we present the chemical potential of the SAD for up to six electrons, extracted from the data shown in Fig. 2. The main frame shows the charging energy, i.e., the difference between the chemical potentials of the interacting and noninteracting systems (the latter is the kinetic energy of the appropriate Fock-Darwin level; see Fig. 1). The transitions in the four-, five-, and six-electron GS's have been marked with open circles. The change of slope for $N=5$ and 6 at 20.5 T is due to the crossing of FD levels (transition in the noninteracting system). As the many-electron GS's are only weakly mixed by the Coulomb interaction, it is useful to think of the N th electron as added to a well defined empty single FD state, but in the presence of a repulsive potential produced by a charge distribution of the $N-1$ initial-state electrons. In Fig. 1 we have indicated the FD states to which the N th electron is added.

The inset in Fig. 3 shows the chemical potential μ , a directly measured quantity. The dashed line shows the energy of the bottom of the WL continuum. We find that only $N=3-4$ electrons can be injected to the dot with energy

below the WL; however, some additional electrons might be transferred into the WL resonances (with energies very well approximated by the higher FD levels⁹). The WL resonances are most likely quite stable due to the energy barrier associated with the drop of the confining potential at the edge of the dot. The maximum number of electrons that can be injected to a dot depends on its size. Taking the dot diameter of 250 Å yields the intershell separation ω_0 actually measured by Drexler *et al.*¹ (≈ 41 meV). For this size we find that the dot can be charged with up to $N=5$ electrons. Note also that the strength of the Coulomb repulsion in the actual SAD is expected to be lower than calculated here due to the finite width of the dot and screening by the electrode. We have checked that taking the 50 Å effective width of the system leads to an approximately 10% decrease in the Coulomb matrix elements.

While in Fig. 3 we have only shown the transitions between the $N-1$ and N electron GS's, for high values of the magnetic field the electrons with the desired spin may not be available in the reservoir (depopulation of Landau levels). Therefore the capacitance spectrum may contain an additional structure due to the magnetic-field-induced transitions in the electron's reservoir, i.e., the metal electrode. Another effect that might lead to new structure not included in Fig. 3 is that the transition probability for charging the ground state vanishes and charging is possible only through an excited N electron state.¹³ The transition probability of the process (for each spin of transferred electron independently) is given by Fermi's golden rule:

$$P_{\sigma}^f \propto \left| \left\langle f \left| \sum_{n,m} c_{nm\sigma}^{\dagger} \right| i \right\rangle \right|^2, \quad (2)$$

where $|i\rangle$ and $|f\rangle$ are the initial ($N-1$ electron) and the final (N electron) states, respectively, and the summation is carried over all bound FD states $|nm\rangle$. In Fig. 4 we present the magnetic-field dependence of charging probabilities P . The energy of the transition is given on the vertical axis and the probabilities of transitions P are proportional to the areas of the circles. As there are no transitions in the GS's of $N=1, 2$, and 3 electrons the corresponding curves follow the noninteracting FD pattern and we showed here only the data for $N \geq 4$. The solid lines give the chemical potential, as in Fig. 3. One can see immediately in Fig. 4 that there is a dramatic difference between the spin-up and spin-down spectra (reflecting the large interlevel spacing) whenever there is a spin gap in the N electron system. In this case the spin-down spectrum does not follow the chemical potential (e.g., for the fields $B > 3$ T and $N=4$). It also appears that for certain ranges of the field the energy of transition does not depend on the spin (excluding the Zeeman splitting), but the probability does, being significantly reduced for the spin-up channel (e.g., for the fields $B < 3$ T and $N=4$).

V. INFRARED SPECTROSCOPY

Infrared (IR) spectroscopy measures excitations spectra of SAD's.¹ The Hamiltonian H_{rad} describing the interaction of the electrons with the IR radiation can be written in the dipole approximation as^{10,14}

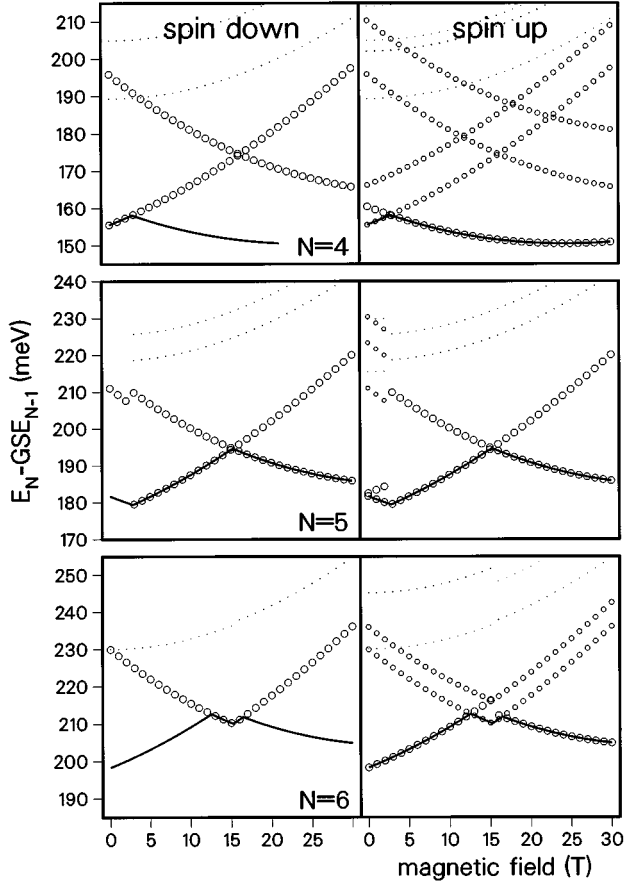


FIG. 4. Evolution of the addition spectrum of SAD's with the magnetic field. The area of the circles is proportional to intensities of transitions. Solid lines give the chemical potential.

$$H_{\text{rad}} = \sum_{i=1}^N \mathbf{r}_i \cdot e \mathbf{E} \exp i \omega t = N \mathbf{R} \cdot e \mathbf{E} \exp i \omega t, \quad (3)$$

where \mathbf{r}_i are coordinates of individual electrons, \mathbf{R} is the center-of-mass (c.m.) coordinate, and $\mathbf{E} \exp i \omega t$ is the electric field uniform over the volume of the dot. For the infinite parabolic confinement only the c.m. excitations with frequencies Ω_+ and Ω_- , independent of the number of electrons (generalized Kohn's theorem),¹⁵ can be measured. The deviations from the ideal parabolic potential introduce new features in the IR spectrum.¹⁴ As shown below, these new structures associated with magnetic-field-induced changes in GS's of SAD's appear in the IR spectrum due to a finite number of confined FD levels.

The IR absorption can be conveniently expressed in terms of the FD ladder operators a and b ^{10,14}:

$$A(\omega) \propto \sum_f \left| \left\langle f \left| \sum_{j=1}^N (a_j + a_j^\dagger + b_j + b_j^\dagger) \right| i \right\rangle \right|^2 \delta(E_f - E_i - \omega), \quad (4)$$

where $|i\rangle$ is the initial (ground) state and the summation goes over all bound final states $|f\rangle$ and over all N electrons. IR radiation connects only the states with the same total spin

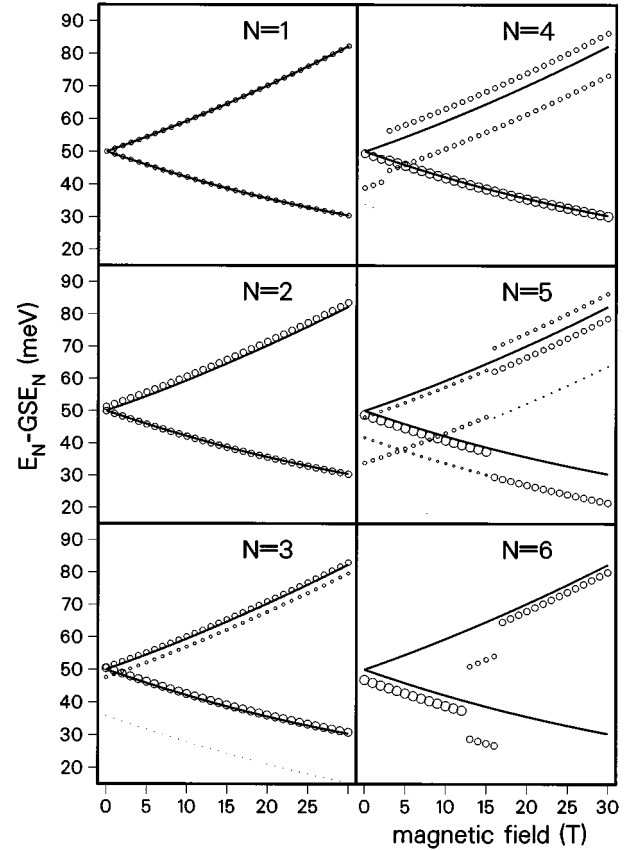


FIG. 5. Evolution of the interlevel excitation spectrum of SAD's with the magnetic field. The area of the circles is proportional to intensities of transitions. Lines give the pure center-of-mass excitations.

and total angular momenta different by ± 1 . We have shown in Fig. 5 the magnetic-field evolutions of the IR spectra calculated for up to six electrons in the SAD. The area of each circle is proportional to the intensity $A(\omega)$. The solid lines show the transition energies Ω_{\pm} of the noninteracting system. We observe deviations from the pure c.m. excitations (a manifestation of the coupling between the c.m. and internal motions), increasing with the number of electrons N . For larger N the small number of available FD states becomes crucial, e.g., there is no six-electron state with $R=7$ available at $B=30$ T and thus no transition with energy $\sim \Omega_-$. These deviations disappear with the inclusion of the increasing number of FD states, that is, with the increase of the size of the dot.

VI. CONCLUSION

We have studied the effect of the electron-electron interaction and the magnetic field on electronic states of lens-shaped self-assembled quantum dots. The charging and infrared spectra of these dots have been calculated and compared with recent experiments by Drexler *et al.* Due to a strong quantization of kinetic energy the Coulomb interaction is treated perturbatively. Nevertheless, the Coulomb interactions and exchange play a crucial role in determining

the Fock-Darwin states observed in charging of partially filled electronic shells. The magnetic-field evolution of the charging and IR spectrum reflects the field-induced transitions in the ground state of the few-electron SAD. We suggest that new information can be obtained by extending magnetic fields up to 30 T.

ACKNOWLEDGMENTS

One of us (P.H.) thanks J. Kotthaus for discussions. A.W. thanks the Institute for Microstructural Sciences, NRC Canada; NATO HTECH, Grant No. 930746; and KBN, Grant No. 202369101, for financial support.

-
- ¹H. Drexler, D. Leonard, W. Hansen, J. P. Kotthaus, and P. M. Petroff, *Phys. Rev. Lett.* **73**, 2252 (1994).
- ²P. M. Petroff and S. P. Denbaars, *Superlatt. Microstruct.* **15**, 15 (1994); for a recent review see *Proceedings of International Conference on Modulated Semiconductor Structures*, Madrid, 1995 [*Solid State Electron.* (to be published)].
- ³M. Grundmann, J. Christen, N. N. Ledentsov, J. Böhrer, D. Bimberg, S. S. Ruvimov, P. Werner, U. Richter, U. Gösele, J. Heydenreich, V. M. Ustinov, A. Yu. Egorov, A. E. Zhukov, P. S. Kopé, and Zh. I. Alferov, *Phys. Rev. Lett.* **74**, 4043 (1995).
- ⁴J.-Y. Marzin, J.-M. Gerard, A. Izrael, D. Barrier, and G. Bastard, *Phys. Rev. Lett.* **73**, 716 (1994).
- ⁵R. Notzel, J. Temmo, A. Kozen, T. Tamamura, T. Fukui, and H. Hasegawa, *Appl. Phys. Lett.* **66**, 2525 (1995).
- ⁶S. Raymond, S. Fafard, P. J. Poole, A. Wojs, P. Hawrylak, S. Charbonneau, D. Leonard, R. Leon, P. M. Petroff, and J. L. Merz (unpublished).
- ⁷R. Leon, S. Fafard, D. Leonard, J. L. Merz, and P. M. Petroff, *Appl. Phys. Lett.* **67**, 521 (1995).
- ⁸D. Leonard, K. Pond, and P. M. Petroff, *Phys. Rev. B* **50**, 11 687 (1994).
- ⁹A. Wojs, P. Hawrylak, S. Fafard, and L. Jacak (unpublished).
- ¹⁰P. Hawrylak, *Solid State Commun.* **88**, 475 (1993).
- ¹¹R. C. Ashoori, H. L. Störmer, J. S. Weiner, L. N. Pfeiffer, K. W. Baldwin, and K. W. West, *Phys. Rev. Lett.* **71**, 613 (1993).
- ¹²P. Hawrylak, *Phys. Rev. Lett.* **71**, 3347 (1993).
- ¹³J. J. Palacios, L. Martin-Moreno, J. H. Oaknin, and C. Tejedor, *Superlatt. Microstruct.* **15**, 91 (1994).
- ¹⁴D. Pfannkuche, V. Gudmundsson, P. Hawrylak, and R. R. Gerhardts, *Solid State Electron.* **37**, 1221 (1994).
- ¹⁵W. Kohn, *Phys. Rev.* **123**, 1242 (1961); L. Brey, N. Johnson, and B. Halperin, *Phys. Rev. B* **40**, 10 647 (1989); P. Maksym and T. Chakraborty, *Phys. Rev. Lett.* **65**, 108 (1990).